Supplemental Material

Supplemental Methods

Transgenic Mice Genotyping

Offspring were genotyped and 3 independent lines were identified for each construct. Mice were genotyped by PCR using tail DNA and primers spanning exon1 and 2 (forward 5'-GGTAGCAATCCTCATCGCTTTC-3') and exon2/3 (reverse 5'-CTTCAGGGTGTTTGCATGCA-3').

Exercise model of physiological hypertrophy

Mice aged 12-16 weeks were swum in a tank (50 cm diameter, ~2000 cm^2 surface area) containing water maintained at 30-32^o C to avoid thermal stress. Mice were initially swum for 10 minutes twice per day, with the sessions separated by a 4 hour break. The swim sessions were increased by 10 minutes each day until the sessions reached a maximum of 90 minutes each, which were maintained for the remainder of the program. The mice were swum 7 days/week for 4 weeks to produce a robust cardiac hypertrophic response (10% increase in HW/BW).[1]

Invasive Hemodynamics

Hemodynamic studies were conducted on mice anesthetized with ketamine (100mg/kg) and xylazine (5mg/kg) and calibrated to keep animals free from distress. The left carotid artery was exposed and a 1.5 Fr SciScience PV loop catheter was advanced into the LV cavity to measure pressure and volume over time. The IVC was occluded to generate a family of pressure-volume curves from which load-independent parameters were derived. The catheter was calibrated using both saline and mouse blood, and the data was analyzed on the AD systems software platform.

Sucrose Gradient Fractionation

Ventricular tissue was rapidly harvested from euthanized mice, flash frozen in liquid nitrogen, and homogenized sequentially in a dounce homogenizer followed by electric

tissue homogenizer (Tissuemizer, Tekmar) in lysis buffer containing 500 mM Na2CO3, 1 mM PMSF, protease inhibitor cocktail (Thermo Scientific), EDTA (1 mM), DTT (1 mM) and beta-glycerophosphate (1 mM). Lysates were nutated at 4 ° C for 60 minutes, sonicated, and then centrifuged (3500 rpm, 10 min, 4 ° C). The pellet was discarded and supernatant protein concentration determined by Bradford assay. An equal amount of protein from each sample was centrifuged for 60 min at 3500 at 4 ° C. Pellets were saved (P1), and supernatants were used for sucrose gradient fractionation after dilution with an equal volume of 80% sucrose (in MBS buffer, final volume 3 ml) and pipetting into SW4 rotor tubes. This was carefully layered with 3 ml of 35% sucrose (in MBS) and finally 5% sucrose (in MBS). Samples were centrifuged for 18 hours at 38,000 rpm. 1 ml fractions were collected from top to bottom, and the pellet (P2, heavy membrane) was solubilized in Lysis buffer containing 1% Triton. Protein concentration of each fraction was determined by Bradford assay. For samples with protein concentration below detection, equal volumes (50 ml) were used for SDS-PAGE. For quantifiable fractions, equal amounts of protein were used for SDS-PAGE.

Whole-cell patch clamp recording

Isolated ventricular myocytes were current and voltage clamped using the whole-cell patch-clamp configuration as previously described[2, 3]. Voltage and current clamp control and data acquisition are performed using custom-written software. Ventricular myocytes were patch-clamped with borosilicate glass electrodes with tip resistances of 3.0~4.0 MΩ when filled with pipette solution. For the measurement of APs, stimulation frequency was varied over cycle lengths of 2.0, 1.0, 0.5 and 0.25 sec, and steady-state APs were recorded and analyzed at least 1 min after pacing at each cycle length in standard Tyrode's solution.

I_{Na} recording was performed at room temperature with patch pipettes of 1-1.5 MΩ tip resistance when filled with pipette solution containing (in mM): NaCl 5, CsCl 40, glutamate 80, CsOH 80, Mg-ATP 5, EGTA 5, HEPES 10, CaCl2 1.5 (free [Ca2+] = 100 nM, pH 7.2 with CsOH, LJP = +5mV). The bath solution contained (in mM) NaCl 10, MgCl2 2, CsCl2 5, TEA-Cl 125, HEPES 20 (pH 7.4 with CsOH). In all experiments, recording was begun 10-15 min after establishment of the whole-cell mode to permit stabilization of current amplitude, voltage dependence and kinetics of gating. Standard voltage protocols were used for assessment of the voltage-dependence of activation/inactivation, recovery from inactivation and entry into inactivation. To determine the membrane potential for V1/2 and the slope factor k, steady state inactivation data were fit with a Boltzmann function of the form: I/Imax= {1+exp[(V-V1/2)/k]}-1. Recovery from inactivation data were fit with a biexponential function of the form: I(t)/Imax=A1·exp(-t/τ1)+A2·exp(-t/τ2)+A3, using a nonlinear least squares minimization. The decay phase of the current during a voltage step was fit with biexponential function of the form: I(t)=Af·exp(-t/τf)+ As·exp(-t/τs), where Af and As are the fractions of fast and slow inactivating components, respectively. Persistent (late) INa was the TTX (30μM)-sensitive currents elicited by 800 ms depolarizations to -20 mV (from -140 mV), from 100-500 ms after depolarizing voltage step normalized to the peak I_{Na}.

The K^+ and Ca^{2+} current measurements were performed at the physiological temperature (37ºC). The detailed patch clamp methods have been described previously (71). In brief, transient outward K+ current (I_{to}) was recorded in Tyrode solution containing 5μmol/l nisoldipine to block ICa. Ito was fitted by a two exponential fit.

Inward rectifier K+ current (I_{K1}) was quantified as the Ba2+-sensitive (0.5 mmol/l) current in the normal Tyrode solution elicited by hyperpolarizing pulse from a holding potential of -40 mV.

Ca^{2+} current (I_{Ca}) was recorded in Tyrode's solution with equimolar replacement of KCl by CsCl, and a pipette solution containing (in mmol/l): 80 Cs-glutamate, 40 CsCl, 10 HEPES, 5 EGTA and 5 Mg-ATP adjusted to pH 7.2 with CsOH.

Histological Characterization

Mid-ventricular short axis heart sections were fixed in 4% paraformaldehyde and 5 mm sections were stained with Masson's trichrome to visualize fibrotic tissue, WGA staining to visualize cardiomyocyte outline, and hematoxylin-eosin to visualize cardiomyocyte architecture. To quantify tissue fibrosis, we used a pre-specified, genotype-blinded image selection methodPercent fibrosis was determined using NIH SCION software to quantitate blue (fibrotic) versus non-blue (non-fibrotic) pixels, and results presented as a percent fibrosis/image area for that entire section. Correlation made with blinded subjective ranking of total fibrosis in hearts visualized at 1.25x, yielded $r=0.75$ ($p<0.05$). Statistical analysis was performed using adjustment for multiple sampling.

REFERENCES

1. Bostrom P, Mann N, Wu J, Quintero PA, Plovie ER, Panakova D, Gupta RK, Xiao C, MacRae CA, Rosenzweig A, Spiegelman BM. C/ebpbeta controls exercise-induced cardiac growth and protects against pathological cardiac remodeling. *Cell*. 2010;143:1072-1083
2. Kaab S, Nuss HB, Chiamvimonvat N, O'Rourke B, Pak PH, Kass DA, Marban E, Tomaselli GF. Ionic mechanism of action potential prolongation in ventricular myocytes from dogs with pacing-induced heart failure. *Circ Res*. 1996;78:262-273
3. Aiba T, Hesketh GG, Barth AS, Liu T, Daya S, Chakir K, Dimaano VL, Abraham TP, O'Rourke B, Akar FG, Kass DA, Tomaselli GF. Electrophysiological consequences of dyssynchronous heart failure and its restoration by resynchronization therapy. *Circulation*. 2009;119:1220-1230

Supplemental Table 1 Baseline gravimetric and functional data on SGK1 transgenic mice and wild-type littermates.

MALES			
Genotype	WT	CA	DN
HW/BW	4.51 ± 0.62 n=13	4.96 ± 0.96 n=9	4.88 ± 0.54 n=9
HW/TL	7.75 ± 1.24 n=13	7.53 ±1.09 n=9	7.89 ± 0.47 n=9
Wall-Thickness (cm)	0.094 ± 0.011 n=27	.095 ± 0.013 n=10	0.091 ± 0.01 n=18
LVDD (cm)	0.261 ± 0.03 n=27	0.272 ± 0.03 n=10	0.266 ± 0.03 n=18
FS (%)	64 ± 5 n=27	56 ± 8 * n=10	64 ± 4 n=18

TABLE 1: Baseline gravimetric and functional data for young adult (average age 3.5 months) and from SGK1-CA, SGK1-DN TG mice and age-matched WT littermates show a significant but modest decrease in fractional shortening is SGK1-CA but not SGK1-DN mice. HW/BW: Heart weight/Body weight; HW/TL: Heart weight/Tibial length; LVDD: left ventricular end diastolic internal diameter; FS: fractional shortening. *p<0.001; **p<0.05. All ECHOs were done in non-sedated, conscious mice with average heart rates 766±79 (SGK1-CA); 768 ± 39 (SGK1-DN) and 758 ± 34 (WT) (p=NS between groups for HR differences).

Supplemental Table 2 Baseline hemodynamic measurements show mild systolic and diastolic dysfunction in SGK1-CA but not SGK1-DN transgenic mice compared to wild-type littermates.

	Wild-type (mean ± SD) n=4	**SGK1-CA (mean ± SD) n=4**	**SGK1-DN (mean ± SD) n=3**
dP/dt_{MAX}(mmHg/sec)	6396 ± 1049	4725 ± 1044*	6538 ± 67.88
dP/dt_{MIN}(mmHg/sec)	-6277 ± 763	-4869 ± 890*	-5354 ± 449
Pre-load Recruitable Stroke Work (mmHg)	82 ±10	60 ± 17*	88.21 ± 2.72
Tau-G (msec)	12.51 ± 1.44	15.39 ± 2.36*	11.31 ± 0.60
Stoke Volume (μL)	21.6 ± 1.95	12.3 ± 5.06*	

Supplementary Table 2: Baseline hemodynamic parameters derived from invasive left ventricular catheterization using a pressure-volume Sci-sense catheter in adult 12-15 week male mice (genotype as indicated). *p ≤ 0.05 versus WT.

Supplemental Table 3: Functional effects of SGK1 activation on the kinetics of sodium current.

	WT	**SGK1-CA**
Activation: $V_{1/2}$, k (mV)	-58.8 ±4.4, 2.0 ±0.6	-68.1 ±3.9**, 2.1 ±0.3
Steady state inactivation: $V_{1/2}$, k (mV)	-77.8 ±4.2, 4.2 ±0.4	-83.9 ±3.6* , 4.6 ±0.7
Recovery from inactivation; τ_{fast}, τ_{slow}	4.4 ±2.1, 55.1 ±19.8	4.0 ±1.7, 84.9 ±48.2
Entry into Inactivation y0	0.84 ±0.06	0.82 ±0.07
A	0.14 ±0.06	0.15 ±0.07
τ	492 ±199	705 ±275

Supplemental Table 3. Functional effects of SGK1 activation on Na^+ current. Calculated parameters of voltage-dependent activation, steady state inactivation, recovery from inactivation and entry into inactivation from whole cell patch clamp of adult ventricular CMs isolated from adult male SGK1-CA TG mice or age-matched WT littermates. The development of intermediate inactivation was fitted with single exponential functions: $y(t) = y0 + A \cdot \exp(-t/\tau)$. * p<0.05 vs. WT, **p<0.01 vs. WT.

Supplemental Figure 1

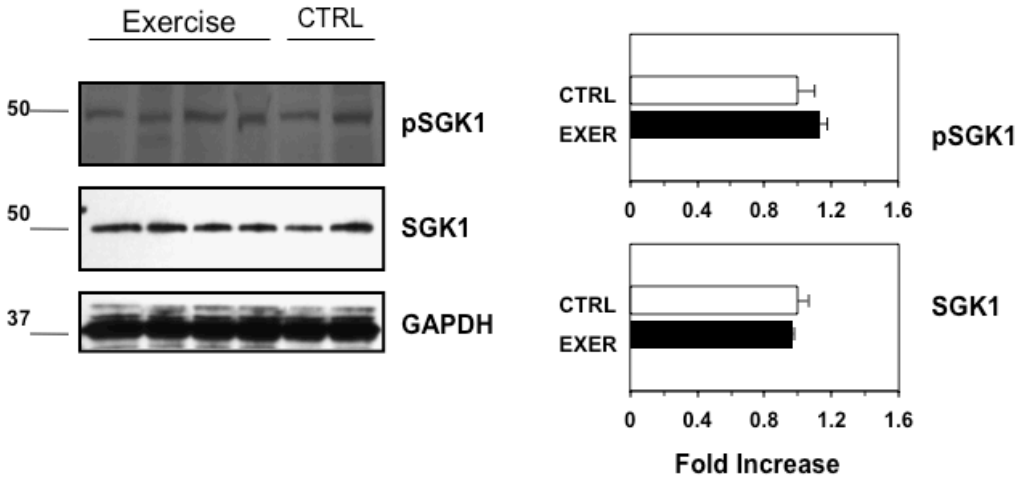

Supplemental Figure 1. SGK1 is not activated in an exercise model of physiological cardiac growth. Western blotting of protein lysates from mice subjected to 4 weeks of exercise (ramp protocol swim training), which exhibited 10% increase in HW/BW ratios or control mice with SGK1 or pSGK1 antibodies. Data are mean±SEM from 3-5 biological replicates per group. p=NS between the groups.

Supplemental Figure 2

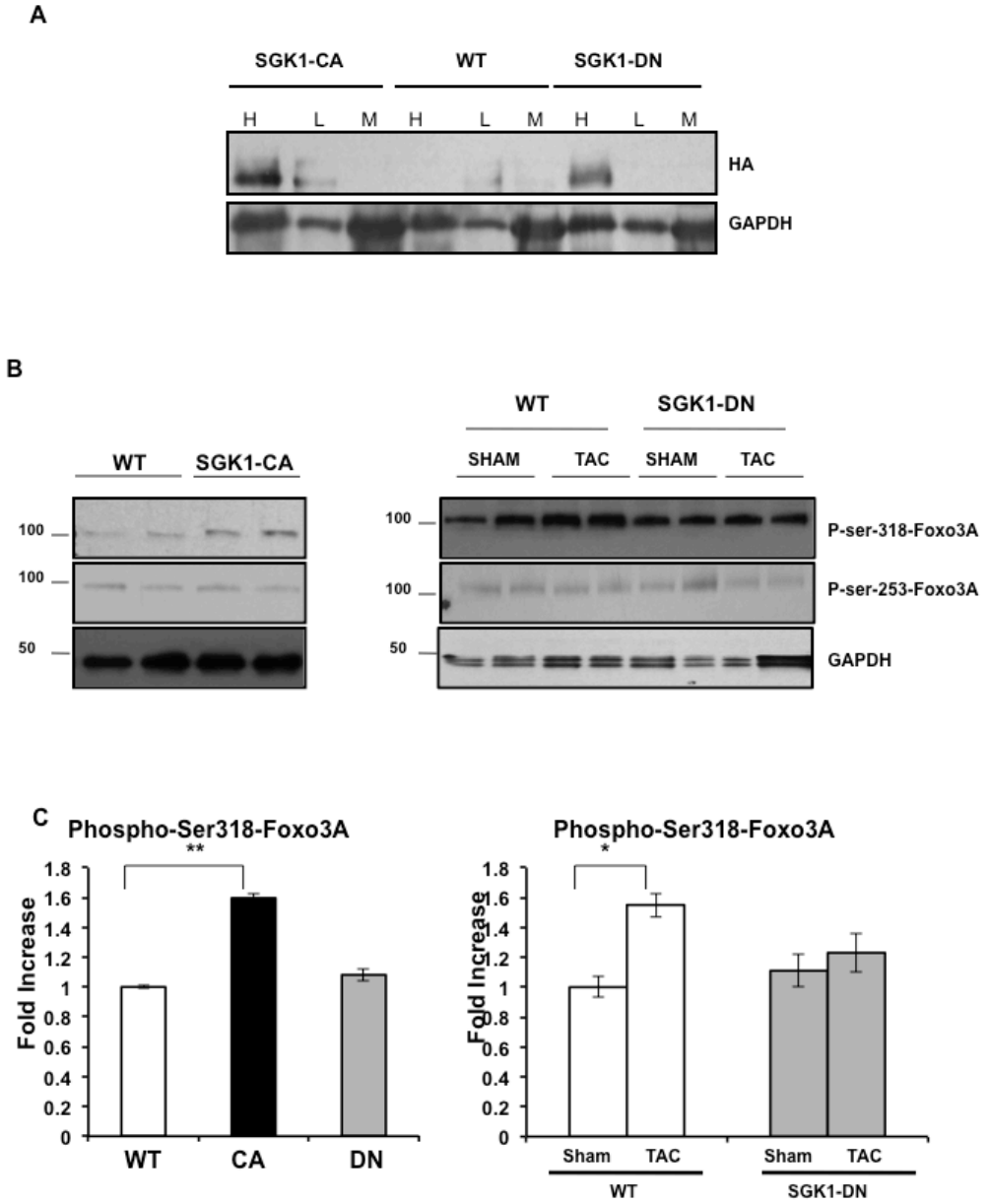

Supplemental Figure 2. Biochemical characterization of SGK1-CA and -DN transgenic mice **(A)** Expression of the HA-tagged transgene as determined by immunoblotting on protein lysates from heart (H), lung (L) or skeletal muscle (M) from SGK1-CA, wild-type (WT) or SGK-DN mice. **(B)** Phosphorylation of the SGK1-specific site Ser318 in Foxo3A is increased at baseline in SGK1-CA hearts and reduced after TAC in SGK1-DN hearts, while the Akt-specific site phospho-(ser253) in Foxo3A is not affected. **(C)** Quantification of phospho(ser318)Foxo3A immunoblot data (normalized to GAPDH) is shown. Fold change is relative to WT sham-operated hearts. *p<0.05, **p<0.01. p=NS for (ser253) Foxo3A (data not shown). Data are mean±SEM of values from 4-6 independent experiments.

Supplemental Figure 3.

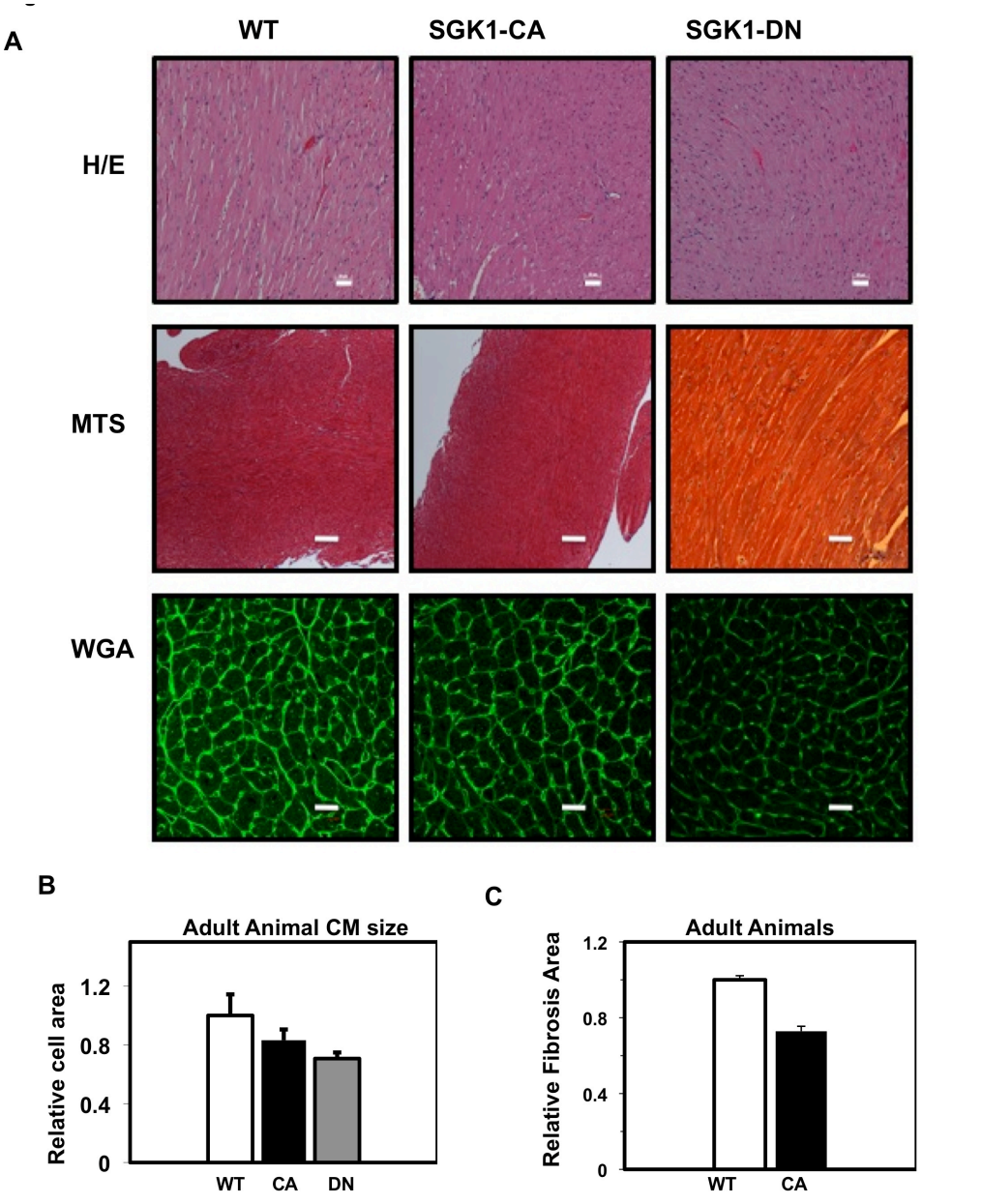

Supplemental Figure 3. Baseline histological analysis of SGK1-CA and -DN transgenic mice. **(A)** Baseline hematoxylin/eosin (H/E), Mason-Trichrome stain (MTS) for fibrosis (blue) and Wheat Germ Agglutinin (WGA) staining for outlining cardiomyocytes in 3-6 month old wild-type (WT), SGK1-CA, or SGK1-DN mice. All images are magnified at 20X, scale bar 50 μm, except for MTS images (10X, scale bar 100 μm). **(B)** Quantification of cardiomyocyte size determined by tracing outlines of WGA stained CMs shown in panel **A** (p=NS by ANOVA between WT and transgenic mice, n=3-4 mice for each group). **(C)** Quantification of fibrosis by Cell-profiler program in adult SGK1-CA mice relative to WT mice (n=3 mice each); p=NS for baseline fibrosis.

Supplemental Figure 4

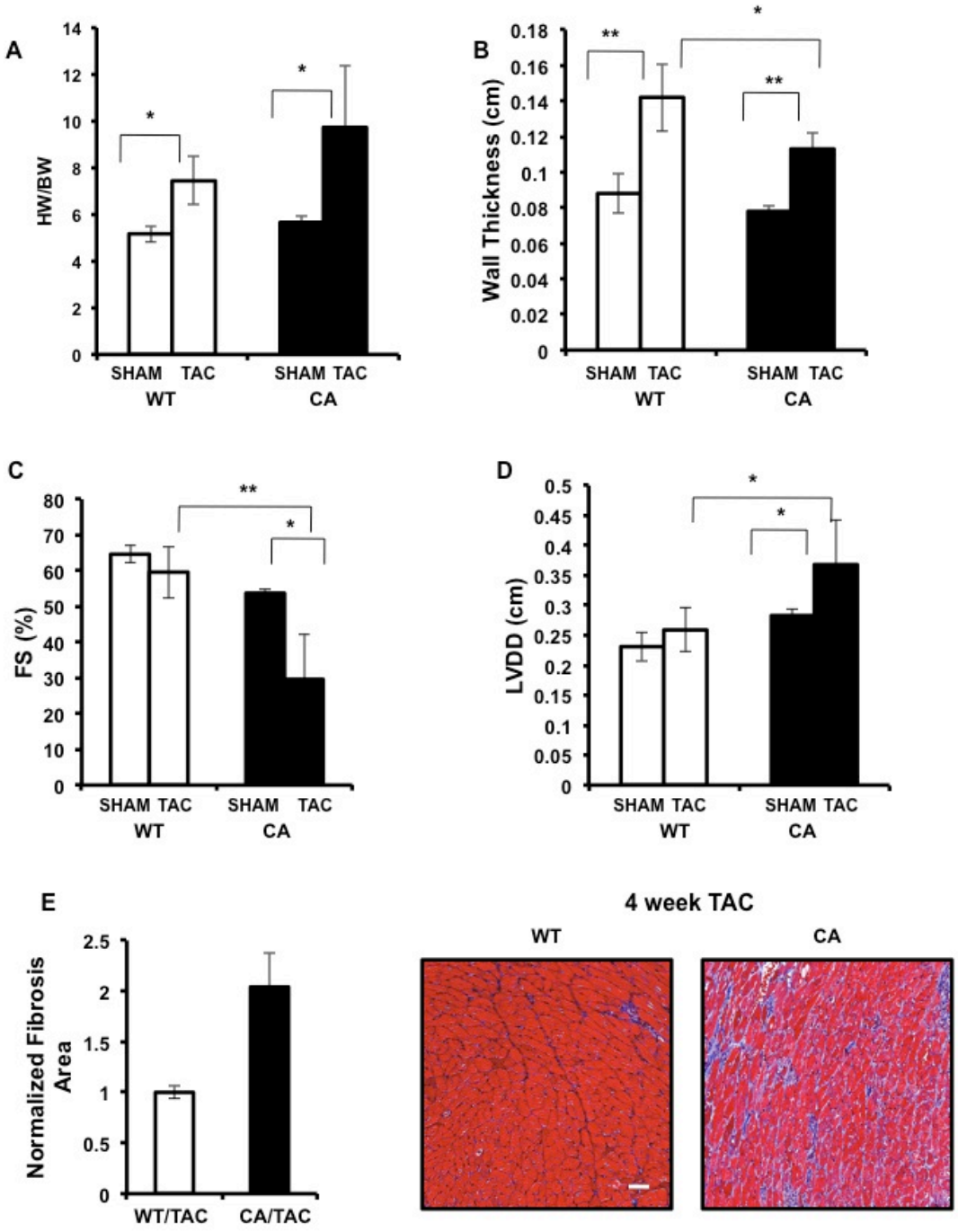

Supplemental Figure 4. Accelerated progression to heart failure in SGK1-CA mice after aortic constriction. **(A-E)**: Gravimetric, echocardiographic, and histologic data from SGK1-CA and WT littermates 4 weeks after TAC or SHAM surgery. **(A)** Heart weight to Body weight ratios (HW/BW) are increased in both SGK1-CA and WT mice; **(B-D)**: Wall thickness, Fractional Shortening (FS), and Left Ventricular Diastolic Dimension (LVDD) showed LV dilatation and decreased function in SGK1-CA mice after TAC compared with post-TAC WT or Sham-operated mice, *p<0.05; **p<0.01; n=5 in TAC groups, n=3 in sham groups **(E)**: Quantification of fibrosis (inset shows representative Masson-Trichrome staining) was not statistically different between SGK1-CA and WT mice after TAC (p=0.1, n=4).

Supplemental Figure 5.

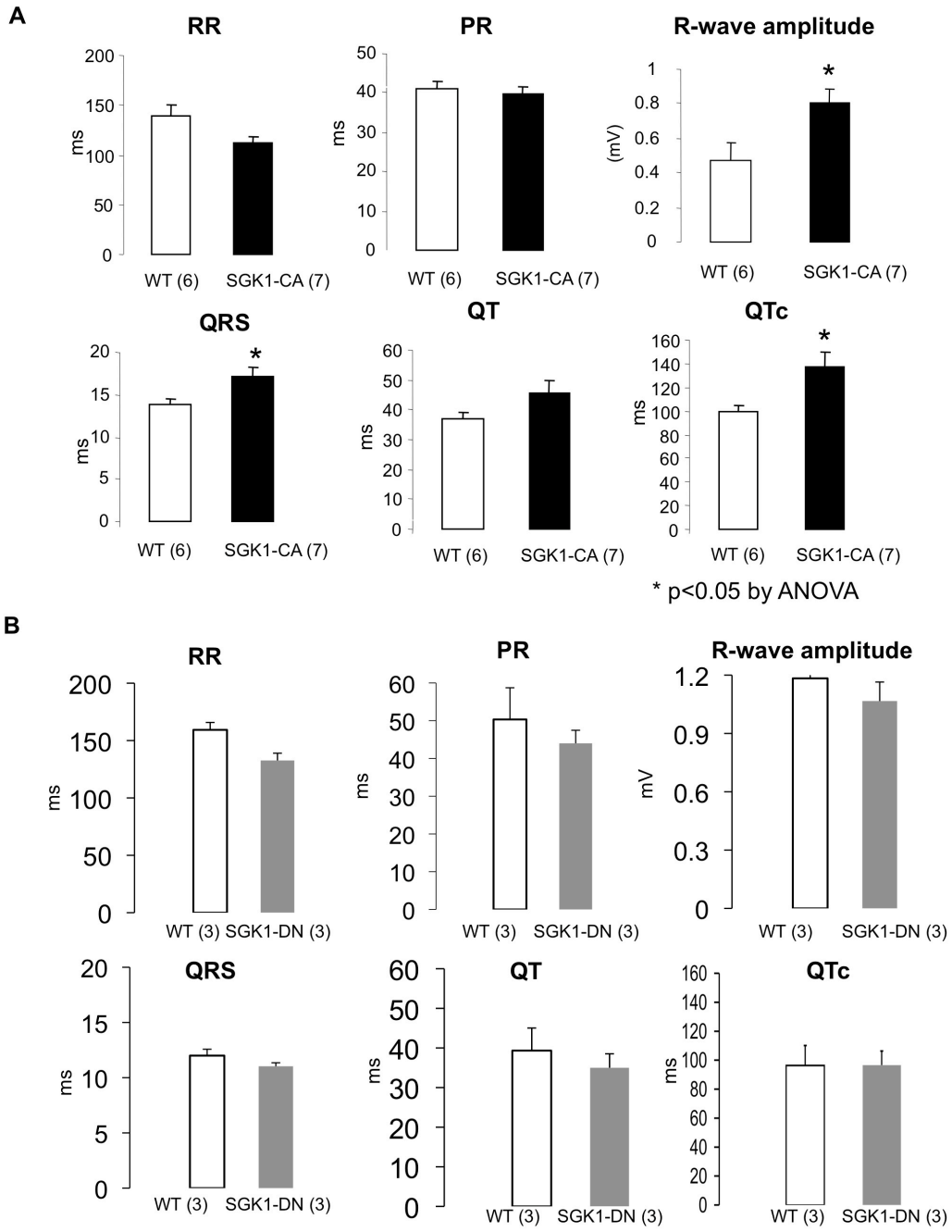

Supplemental Figure 5. Baseline electrocardiography in transgenic mice and wild-type littermates. Comparison of baseline electrocardiographic characteristics of SGK1-CA and WT littermates **(A)**; and SGK1-DN and WT littermates **(B)**. *p<0.05 by ANOVA. The recording amplifier and needle electrodes used in the SGK1-DN mice were different from the ones used for the SGK1-CA mice, and hence the R wave amplitudes cannot be compared between panel A and panel B.

Supplemental Figure 6

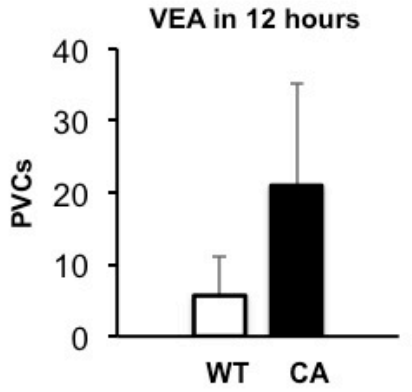

Supplemental Figure 6. Holter monitoring in SGK1-CA TG mice. SGK1-CA TG mice or WT littermates were subjected to implantable Holter monitoring for 7 days. While no sudden death was recorded, there was a trend towards increased PVC in SGK1-CA mice.

Supplemental Figure 7

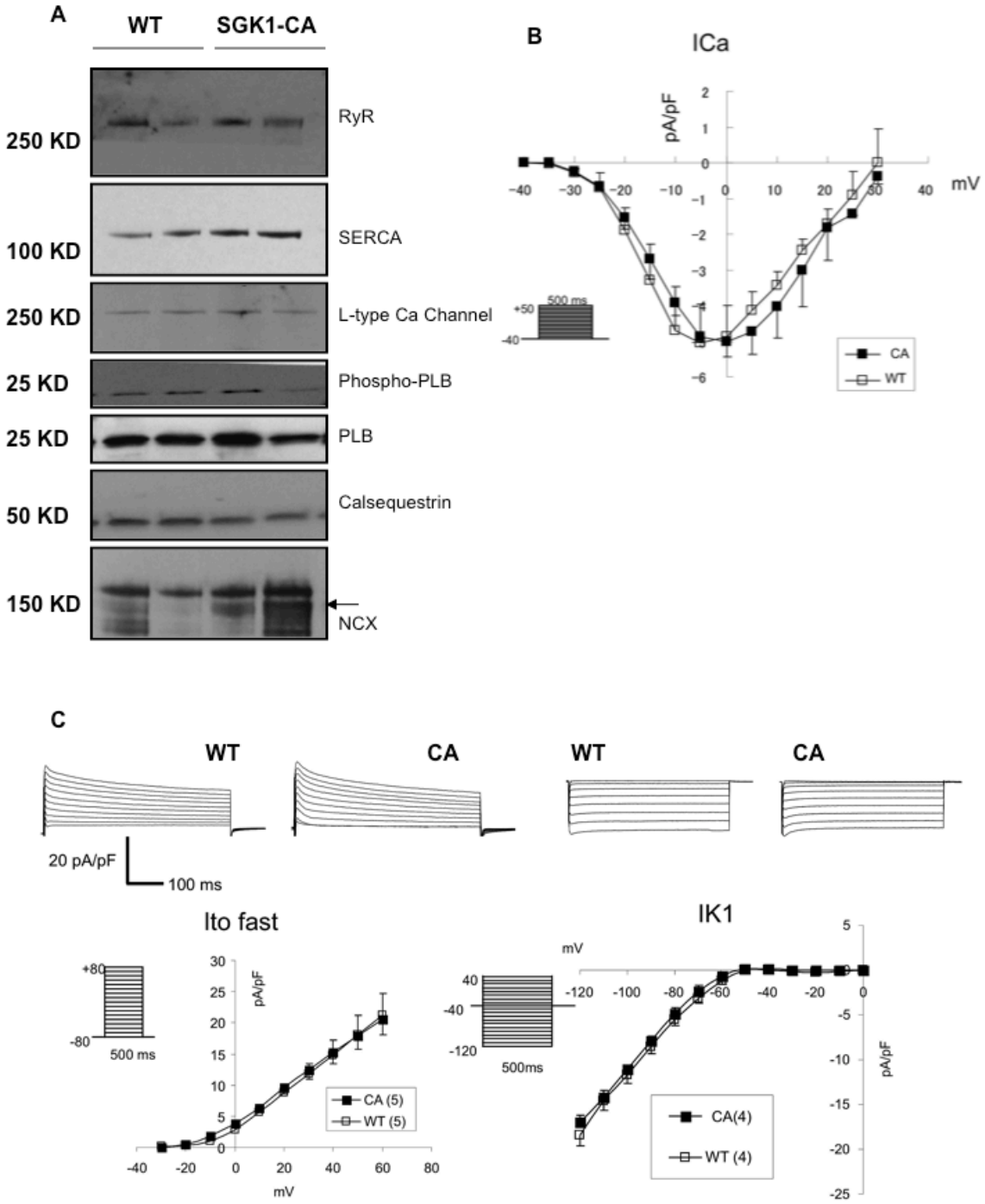

Supplemental Figure 7. Calcium handling proteins, potassium and calcium currents in SGK1-CA mice. **(A)** Immunoblotting of membrane fractions from SGK1-CA and WT mice (4-6 each) show an increase in the Na^+-Ca^{2+}-exchanger (NCX) (p=0.01) but not other calcium-handling proteins. Data is normalized to GAPDH expression and shown as fold increase over WT expression levels (mean±SEM, 3 experiments each). **(B)** The peak I-V relationships for I_{Ca} in WT and SGK1-CA myocytes showed no significant difference. **(C)** Representative I_{to} currents (left, top) and peak I-V relationship of I_{to} fast in each group (left, bottom) in myocytes from WT and SGK1-CA mice (voltage-clamp protocol shown in inset). Representative I_{K1} current traces (right, top) and steady state current-voltage (I-V) relationship of I_{K1} in each group (right, bottom) in the WT and SGK1-CA mice elicited by the voltage-clamp protocol shown in the inset. No significant difference was found in the I_{to} and I_{K1} between WT and SGK1-CA myocytes.

Supplemental Figure 8.

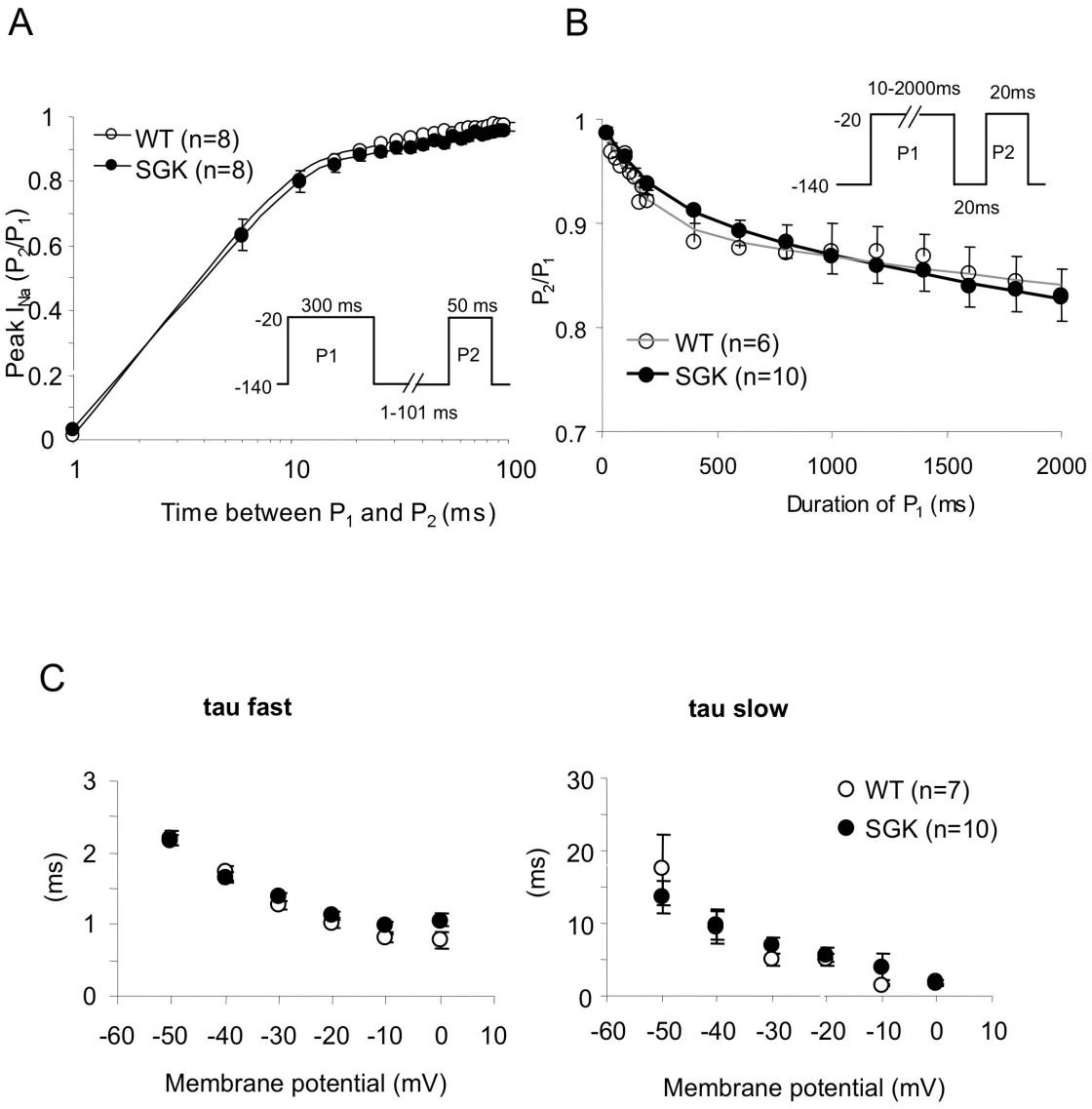

Supplemental Figure 8. Recovery from inactivation, entry into slow inactivation, and decay of I_{Na} in WT and SGK1-CA mice. **(A)** Recovery from inactivation of I_{Na} in WT and SGK1-CA mice cardiomyocytes is not different. Recovery data are fit to double exponential functions. **(B)** Kinetics of entry into slow inactivated states of I_{Na} in WT and SGK1-CA mice CMs are unaltered. Mean data are fit to double exponential function. **(C)** The fast and slow components of I_{Na} decay in WT and SGK-TG cardiomyocytes are superimposable over a range of voltages. I_{Na} decay was fit with a double exponential.

Supplemental Figure 9

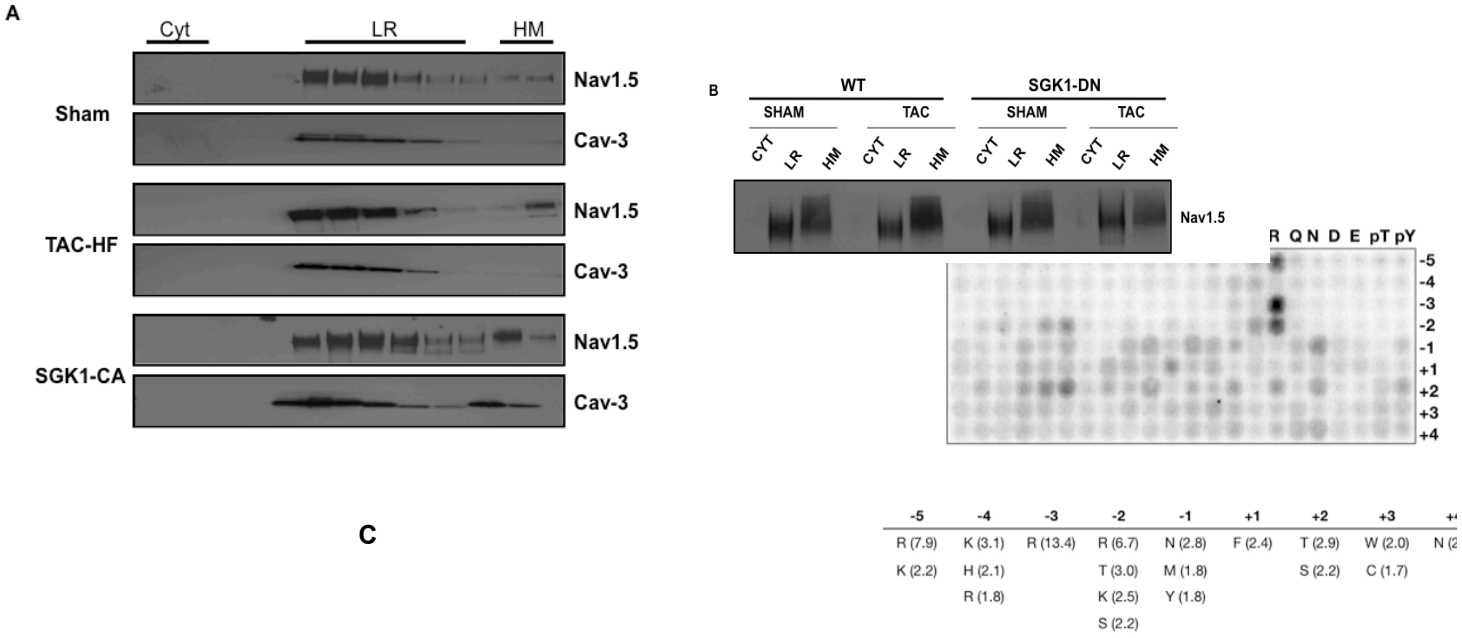

D

Candidate SGK1 Phosphorylation Targets in SCN5a

Score	Domain	Site	Sequence
0.671	I-II linker	S664	GARQRAL**S**AVSVLTS
0.6818	SH3BP5/I-II linker	S484	KRRKRLS**S**GTEDGGD
0.6983	SH3BP5/I-II linker	S483	SKRRKRL**S**SGTEDGG
0.8233	N-terminus	S36	AEKQARG**S**ATSQESR
0.8369	Transmembrane(D4/S3)	T1590	ALRHYYF**T**NSWNIFD

Supplemental Figure 9: Interaction of SGK1 with Nav 1.5. **(A)** Representative sucrose gradients from WT sham-operated animals (sham), WT mice with TAC-induced heart failure (TAC-HF), or unoperated SGK1-CA mice, were immunoblotted for Nav1.5 or caveolin-3 (cav-3, to mark lipid raft). Nav1.5 in the heavy membrane (HM) fraction is increased in SGK1-CA and TAC-HF. (Cyt: cytoplasmic; LR: lipid raft; HM: heavy membrane; 3 animals in each group). **(B)** Indicated sucrose gradient fractions from WT or SGK1-DN mice after TAC or sham-operation were pooled and immunoblotted with Nav1.5 antibody. The increased Nav1.5 in HM after TAC in WT mice is not seen in SGK1-DN mice after TAC. **(C)** Autoradiographic exposure of 20μg of recombinant SGK1 reacted with a peptide library mixture where 1 of 20 naturally occurring amino acids is fixed at 9 positions surrounding a serine or threonine residue. The amount of radiolabeled ATP incorporation is averaged and data are normalized for each amino acid. An average value greater or less than 1 represents positive or negative selectivity, respectively. The sequence preference of phosphorylation by SGK1 for 9 fixed positions (-5 to +4) surrounding a serine or threonine is listed. **(D)** The table below shows the top 5 Nav 1.5 phosphorylation sites. Peptide targets identified by Scansite using the vertebrate Swiss-Prot database. A lower score indicates a higher likelihood of SGK1 phosphorylation at that site.